Excitonic Dynamical Franz-Keldysh Effect

K. B. Nordstrom,[1] K. Johnsen,[2,3] S. J. Allen,[1] A.-P. Jauho,[2] B. Birnir,[3] J. Kono,[4] T. Noda,[5]
H. Akiyama,[5] and H. Sakaki[4,5]
[1]*Center for Terahertz Science and Technology, Quantum Institute, University of California, Santa Barbara, California 93106*
[2]*Mikroelektronik Centret, Technical University of Denmark, Bldg 345east, DK-2800 Lyngby, Denmark*
[3]*Mathematics Department, University of California, Santa Barbara, California 93106*
[4]*Quantum Transition Project, Japan Science & Technology Corporation, Tokyo 153, Japan*
[5]*Institute of Industrial Science, University of Tokyo, Tokyo 106, Japan*
(Received 30 December 1997)

The dynamical Franz-Keldysh effect is exposed by exploring near-band-gap absorption in the presence of intense THz electric fields. It bridges the gap between the dc Franz-Keldysh effect and multiphoton absorption and competes with the THz ac Stark effect in shifting the energy of the excitonic resonance. A theoretical model which includes the strong THz field nonperturbatively via a nonequilibrium Green functions technique is able to describe the dynamical Franz-Keldysh effect in the presence of excitonic absorption. [S0031-9007(98)06611-3]

PACS numbers: 78.30.Fs, 71.35.Cc, 78.20.Bh, 78.66.Fd

We report observation of the dynamical Franz-Keldysh effect (DFKE) by examination of the near-band-gap optical properties of a semiconductor multiple quantum well (MQW) in a new experimental regime. By applying a strong electric field at frequencies near 1 THz, we perform electroabsorption spectroscopy which is described neither by the dc Franz-Keldysh effect (FKE) [1,2] nor by optical-frequency effects like multiphoton absorption (MPA) [3]. The DFKE region, bridging these two extremes, is a topic of long-standing theoretical interest [4–6], but has not previously been studied experimentally.

The crossover between "high" and "low" frequency may be quantified in terms of two parameters, E_{KE} and γ, defined as

$$E_{\mathrm{KE}} = \frac{e^2 E_{\mathrm{THz}}^2}{4m^* \omega_{\mathrm{THz}}^2}. \tag{1}$$

$$\gamma = \frac{E_{\mathrm{KE}}}{\hbar\omega_{\mathrm{THz}}} = \frac{e^2 E_{\mathrm{THz}}^2}{4m^* \hbar \omega_{\mathrm{THz}}^3}. \tag{2}$$

E_{KE} is the mean kinetic energy of a particle of mass m^* and charge e in an electric field $\vec{E}_{\mathrm{THz}} \cos(\omega_{\mathrm{THz}} t)$, i.e., the ponderomotive energy. The dc FKE corresponds to $\gamma \gg 1$; multiphoton effects occur for $\gamma \ll 1$; and the case of $\gamma \sim 1$ is a new, distinct DFKE regime [4] (Fig. 1). This regime is difficult to access experimentally, as E_{KE} must be comparable to or greater than any broadening energies in the system. However, it is possible for applied fields with $\omega_{\mathrm{THz}} \sim 1$ THz and $E_{\mathrm{THz}} \sim 1$–10 kV/cm [5].

In this paper, we explore the optical absorption of a semiconductor MQW driven by an intense THz electric field polarized in the plane of the MQW layers. For the case of noninteracting carriers, the DFKE predicts a blueshift of the main absorption edge in the spectrum by E_{KE}, as well as increased subgap absorption [5] (Fig. 2a). This DFKE blueshift has not previously been observed.

In order to properly address the DFKE, we must also consider the effect of excitons, which dominate the observed near-band-gap absorption in undoped semiconductors. Excitons are bound states of an electron and hole with hydrogenlike quantized energy levels. The energy level spacings can be in the THz regime. The interaction of excitonic states with a THz field leads to shifts of the levels via the ac Stark effect [7] (Fig. 2b). The THz field interacts most strongly with the exciton $1s \rightarrow 2p$ transition [8]. We present below a novel theoretical model which shows that the experimentally observed changes in the absorption spectrum, as a function of the THz field intensity and frequency, display the DFKE and its interplay with the ac Stark effect.

Our MBE-grown sample consists of a 20-period MQW with 80 Å $In_{0.2}Ga_{0.8}As$ wells separated by 150 Å GaAs barriers on a GaAs substrate. The energy of the 2D MQW states is below the substrate band gap, allowing us to perform direct transmission spectroscopy without substrate removal. Strain lifts the valence-band degeneracy at $k = 0$, splitting the light-hole and heavy-hole bands by

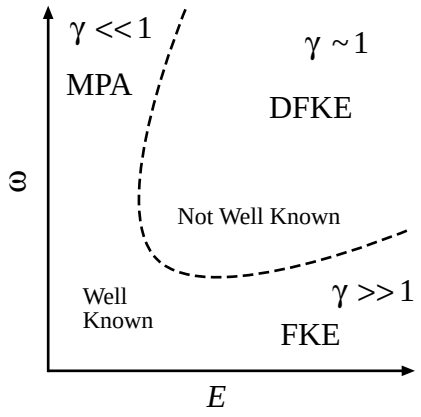

FIG. 1. A schematic map of electro-optic phase space as a function of amplitude and frequency of the perturbing field, showing DFKE regime "between" MPA and FKE.

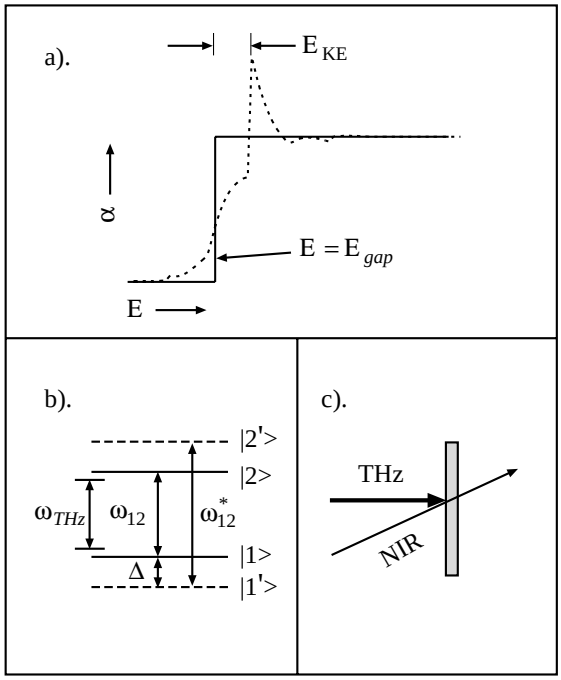

FIG. 2. (a) DFKE in an ideal 2D system. In a strong THz field (dashed curve, solid curve is zero field), the "edge" shifts to higher frequency and subgap absorption increases. (b) The ac Stark effect: a strong field applied at frequency $\omega \sim \omega_{12}$ causes ω_{12} to shift. For $\omega < (>)\omega_{12}$, the transition shifts to $\omega_{12}^{*} > (<)\omega_{12}$. $\Delta = (\omega_{12} - \omega_{12}^{*})/2$ is the shift of $|1\rangle$ with respect to distant energy levels. (c) Schematic of experiment.

50 meV. The electron-heavy-hole exciton is the lowest-energy feature. It is inhomogeneously broadened by interface roughness and alloy disorder [9] with a FWHM of 6 meV. The exciton $1s \rightarrow 2p$ transition energy ($\hbar\omega_{12}$) is ~8 meV, estimated from magnetotransmission experiments [8].

A cw Ti-sapphire laser provides tunable near-band-gap radiation, in the near infrared (NIR), focused to an ~200 μm spot. Its transmission is detected by a conventional Si p-i-n photodiode, and peak NIR intensity is ~100 mW/cm^2. THz radiation is provided by the UCSB free-electron laser, a source of intense, coherent radiation tunable from $\hbar\omega_{\mathrm{THz}} \sim 0.5$–$20$ meV [10]. It is roughly collinear with the NIR beam and focused to a 0.5–2.5 mm spot coincident with the NIR focus (Fig. 2c). We measure transmission spectra as a function of THz intensity and frequency. All measurements are performed in He vapor at ~7 K.

We observe two distinct regimes of experimental behavior for different ranges of THz frequency, ω_{THz}. When ω_{THz} is less than ω_{12}, we observe a redshift of the exciton for low THz intensities, i.e., an ac Stark shift. As THz intensity increases, this shift reaches a maximum and reverses, eventually becoming a net blueshift at the highest THz intensity; the DFKE blueshift dominates at high intensities as the ac Stark effect saturates (Fig. 3a). Conversely, if ω_{THz} is greater than ω_{12}, we observe a blueshift of the exciton which increases monotonically with increasing THz intensity; the ac Stark effect and DFKE act in concert, each contributing to the blueshift (Fig. 3b). In both cases, the exciton peak is broadened and suppressed, and the broadening increases with increased THz intensity (Figs. 3a and 3b).

Since the apparent peak shifts are small, we quantify them by taking a weighted average of the data near the exciton line. We find the geometric mean of the upper half of the excitonic peak, and plot this "center of mass" against γ, which is directly proportional to THz power (Fig. 4). Note that our estimates of the maximum γ at each frequency are only accurate to within a factor of 2 or 3. We also show results of our theoretical calculations (to be discussed below). Again, we see an initial redshift, followed by a blueshift at low ω_{THz} (Fig. 4a) and a monotonic blueshift at high ω_{THz} (Fig. 4b).

Theoretically, we describe the optical properties of the system by calculating the time dependent induced polarization. The system is probed using a weak NIR probe field $\vec{E}_{\mathrm{NIR}}(t)$ with frequency $\omega \sim E_{\mathrm{gap}}/\hbar$. To linear order in the NIR field, the macroscopic polarization is the $\vec{k}$ trace of

$$\vec{P}(\vec{k},t) = \int_{-\infty}^{\infty} dt'\, \chi^{r}(\vec{k};t,t')\vec{E}_{\mathrm{NIR}}(t')\,. \qquad (3)$$

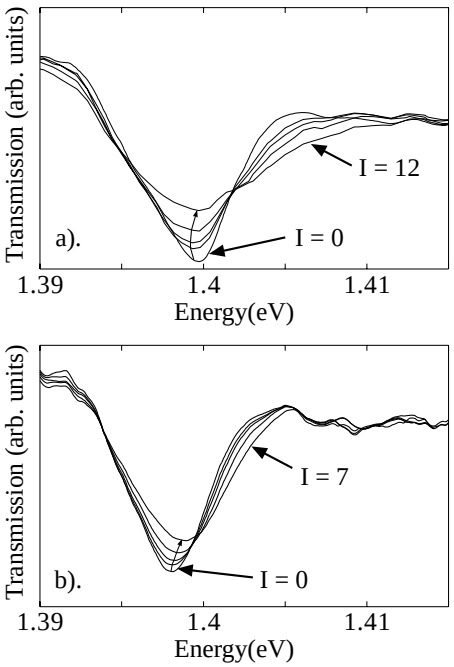

FIG. 3. Experimental transmission of MQW near e1h1 exciton with (a) $\hbar\omega_{\mathrm{THz}} = 2.5$ meV at $I_{\mathrm{THz}} = 0, 1, 2, 4, 12$ (arbitrary units). (b) $\hbar\omega_{\mathrm{THz}} = 14$ meV at $I_{\mathrm{THz}} = 0, 1, 2, 4, 7$ (arbitrary units). Arrows connect calculated centers of experimental peaks and point in the direction of increasing I_{THz}.

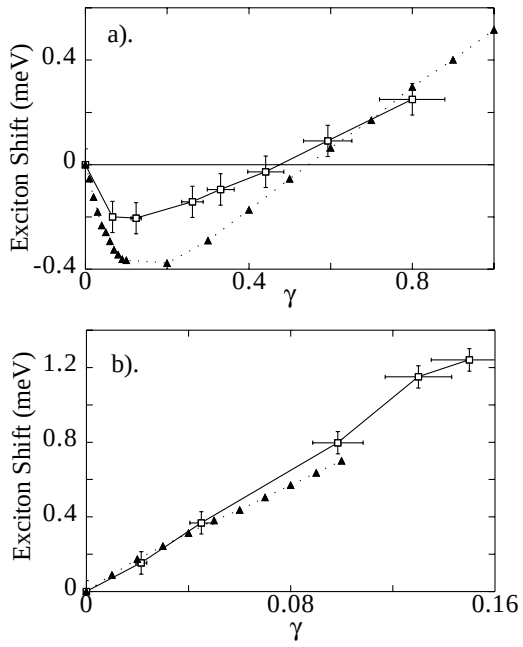

FIG. 4. Center of mass of measured (squares) and calculated (triangles) exciton transmission peak vs γ for (a) $\hbar\omega_{\mathrm{THz}} = 2.5$ meV $< \hbar\omega_{12}$ and (b) $\hbar\omega_{\mathrm{THz}} = 10.5$ meV $> \hbar\omega_{12}$.

All the information about the THz field is contained in the nonequilibrium generalization of the retarded two-time interband susceptibility $\chi^r(\vec{k}; t, t')$. In our previous work [5], based on nonequilibrium Green functions, we studied the susceptibility starting from a two-band Hamiltonian, including the THz field nonperturbatively in the Coulomb gauge via the vector potential $\vec{A}(t) = -\vec{E}_{\mathrm{THz}} \sin(\omega_{\mathrm{THz}} t)/\omega_{\mathrm{THz}}$. Here, $\vec{E}_{\mathrm{THz}}$ is oriented in the plane of the MQW layers. Nonequilibrium Green function techniques [11] yield an analytic expression for the single particle susceptibility:

$$\bar{\chi}^r(\vec{k}; t, t') = -\frac{2d^2}{\hbar}\,\theta(t - t')\sin\left\{\int_{t'}^{t} \frac{ds}{\hbar}\,\epsilon[\hbar\vec{k} - e\vec{A}(s)]\right\}, \tag{4}$$

where d is a dipole matrix element and $\epsilon[\vec{k}] = \frac{k^2}{2\mu} + E_{\mathrm{gap}}$, μ being the electron-hole reduced mass and $\vec{k}$ the in-plane momentum.

We include excitonic effects by using the Bethe-Salpeter equation [12] to determine a susceptibility which includes the electron-hole interaction in the ladder approximation,

$$\chi^r(\vec{k}; t, t') = \bar{\chi}^r(\vec{k}; t, t') + \int \frac{d^2\vec{k}'}{(2\pi)^2} \int_{-\infty}^{\infty} dt''\, \bar{\chi}^r(\vec{k}; t, t'') \times V(|\vec{k} - \vec{k}'|)\chi^r(\vec{k}'; t'', t'), \tag{5}$$

where $\bar{\chi}^r(\vec{k}; t, t')$ is the single-particle, noninteracting susceptibility of Eq. (4). Expressing the susceptibility as $\chi^r(\vec{k}; t, t') = \sum_n \int \frac{d\omega}{2\pi}\, \chi_n^r(\vec{k}, \omega) e^{i\omega(t-t') + in2\omega_{\mathrm{THz}}(t+t')}$, the integral equation (5) becomes a matrix equation [13],

$$\chi_n^r(\vec{k}, \omega) = \bar{\chi}_n^r(\vec{k}, \omega) + \sum_{n'} \bar{\chi}_{n-n'}^r(\vec{k}, \omega + 2n'\omega_{\mathrm{THz}}) \int \frac{d^2\vec{k}'}{(2\pi)^2}\, V(|\vec{k} - \vec{k}'|)\chi_{n'}^r[\vec{k}', \omega + 2(n' - n)\omega_{\mathrm{THz}}]. \tag{6}$$

For physically achievable THz intensities, only small values of n are needed.

Numerically, we solve the matrix equation including both s-wave and p-wave scattering; both are important, since the THz field will couple the s and p states of the exciton and influence the observed resonance via the ac Stark effect. The solutions to the resulting equation are found by discretizing the integrals to yield a set of linear equations which we solve by standard methods [14].

Finally, we relate the results to physically measurable quantities by expressing the macroscopic polarization as

$$\vec{P}(t) = \vec{E}_{\mathrm{NIR}} \sum_n \tilde{\chi}_n(\omega) e^{i(2n\omega_{\mathrm{THz}} - \omega)t}, \tag{7}$$

where $\tilde{\chi}_n(\omega) = \sum_{\vec{k}} \chi_n^r(\vec{k}, \omega)$. The linear absorption is thus proportional to Im $\tilde{\chi}_0(\omega)$. The terms with $n \neq 0$ describe the nonlinear mixing of the NIR and the THz field, resulting in optical sideband generation. These sidebands show a rich structure, but an analysis is beyond the scope of this work, and will be reported separately.

Using the above method, we have calculated absorption spectra using the experimental parameters of our system. We find good agreement with experiment, using no fitted parameters. For $\omega_{\mathrm{THz}} < \omega_{12}$, theory predicts a redshift of the exciton absorption peak at low THz intensities. With increasing THz intensity, the shift saturates and then reverses, eventually becoming a net blueshift (Fig. 5a). Theory also predicts a blueshift for $\omega_{\mathrm{THz}} > \omega_{12}$, which monotonically increases with THz intensity for experimentally accessible intensities (Fig. 5b). In both cases, the exciton peak is suppressed and inhomogeneously broadened with increasing intensity, i.e., with increasing γ (Figs. 5a and 5b). Using the same method as for the measured spectra, we compute the center of mass of the calculated exciton lines. We plot the shift of the theoretical "center of mass" as a function of γ in Fig. 4, along with the experimental results. The theoretical and experimental peak shifts show identical qualitative behavior.

As described above, this behavior can be understood as the DFKE acting in competition with the ac Stark effect. The ac Stark effect, at low E_{THz}, results in a shift of the

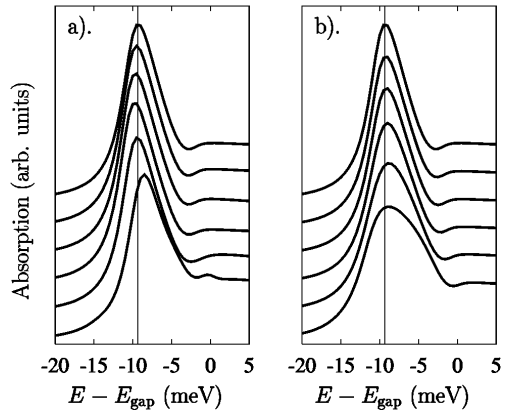

FIG. 5. Calculated absorption of MQW with (a) $\hbar\omega_{THz} = 2.5$ meV $< \hbar\omega_{12}$ from top down at $\gamma = 0$, 0.03, 0.06, 0.1, 0.5, and 1.5. (b) $\hbar\omega_{THz} = 14$ meV $> \hbar\omega_{12}$ from top down at $\gamma = 0$, 0.01, 0.02, 0.04, 0.08, and 0.15.

exciton level,

$$\Delta \propto \frac{(\omega_{THz} - \omega_{12})E_{THz}^2}{(\omega_{THz} - \omega_{12})^2 + \Gamma^2}, \tag{8}$$

where Γ is the width of the $1s \rightarrow 2p$ transition line [7]. We estimate $\hbar\Gamma \sim 4$ meV in our sample. The magnitude of Δ is dominated by Γ, and we expect little resonant enhancement of $|\Delta|$ for $\omega_{THz} \sim \omega_{12}$. Δ does not increase indefinitely, and will saturate as E_{THz} increases, going from quadratic to linear dependence on E_{THz} [7]. The DFKE, however, always provides a blueshift proportional to E_{THz}^2, given by E_{KE} [5].

The net effect is illustrated in Fig. 4, which shows the shift of the center of mass of the exciton transmission peak as a function of γ for both theory and experiment. For $\omega_{THz} < \omega_{12}$, we see a redshift which saturates and reverses with increasing intensity, showing a roughly linear dependence on THz intensity at high fields (Fig. 4a). At low fields, Δ dominates, resulting in a net redshift. As Δ saturates with increasing field, E_{KE} begins to dominate, eventually overwhelming the redshift entirely and resulting in a net blueshift. For $\omega_{THz} > \omega_{12}$, we observe only an increasing blueshift with increasing E_{THz} (Fig. 4b). Here, Δ and E_{KE} cooperate to create a blueshift.

In conclusion, we have observed the experimental signature of DFKE through its interplay with the ac Stark effect. Our theory and observations are in remarkable agreement, and show the resulting frequency- and intensity-dependent shift of the excitonic resonance in a MQW under intense THz irradiation.

This work is supported by ONR Grant No. N00014-92-J-1452, the Quantum Transition Project of JSTC, QUEST (an NSF Science & Technology Center), LACOR Grant No. 4157U0015-3A from Los Alamos National Laboratory, National Science Foundation Grant No. CDA96-01954, and Silicon Graphics, Inc. The authors also thank D. P. Enyeart, D. T. White, J. R. Allen, and G. Ramian at the Center for Terahertz Science & Technology for their invaluable technical support.

[1] W. Franz, Z. Naturforsch. **13**, 484 (1958).
[2] L. V. Keldysh, Sov. Phys. JETP **34**, 788 (1958).
[3] See, e.g., V. Nathan, A. H. Guenther, and S. S. Mitra, J. Opt. Soc. Am. B **2**, 294 (1985), and references therein.
[4] Y. Yacoby, Phys. Rev. **169**, 610 (1968).
[5] A.-P. Jauho and K. Johnsen, Phys. Rev. Lett. **76**, 4576 (1996); K. Johnsen and A.-P. Jauho, Phys. Rev. B **57**, 8860 (1998).
[6] Y. T. Rebane, Sov. Phys. Solid State **27**, 824 (1985).
[7] See, e.g., J. S. Bakos, Phys. Rep. **31C**, 209 (1977), and references therein.
[8] J. Kono, M. Y. Su, T. Inoshita, T. Noda, M. S. Sherwin, S. J. Allen, Jr., and H. Sakaki, Phys. Rev. Lett. **79**, 1758 (1997).
[9] A. Patanè, A. Polimeni, M. Capizzi, and F. Martelli, Phys. Rev. B **52**, 2784 (1995).
[10] G. Ramian, Nucl. Instrum. Methods Phys. Res., Sect. A **318**, 225 (1992).
[11] H. Haug and A.-P. Jauho, *Quantum Kinetics in Transport and Optics of Semiconductors,* Springer Series in Solid-State Sciences Vol. 123 (Springer, Berlin, 1996).
[12] H. Haug and S. Schmitt-Rink, Prog. Quantum Electron. **9**, 1 (1984).
[13] K. Johnsen and A.-P. Jauho (unpublished).
[14] H. Haug and S. W. Koch, *Quantum Theory of the Optical and Electronic Properties of Semiconductors* (World Scientific, Singapore, 1993).